mathematics

Article

Extension Distance-Driven K-Means: A Novel Clustering Framework for Fan-Shaped Data Distributions

Xingsen Li ^{1,†}, Hanqi Yue ^{1,†}, Yaocong Qin ^{1,*,†} and Haolan Zhang ^{2,*,†}

[1] Research Institute of Extenics and Innovation, Guangdong University of Technology, Guangzhou 510006, China; lixs@gdut.edu.cn (X.L.); luckyq057@163.com (H.Y.)
[2] College of Computer and Data Engineering, NingboTech University, Ningbo 315104, China
[*] Correspondence: 16638687331@163.com (Y.Q.); haolan.zhang@nit.zju.edu.cn (H.Z.)
[†] These authors contributed equally to this work.

Abstract

The K-means algorithm utilizes the Euclidean distance metric to quantify the similarity between data points and clusters, with the fundamental objective of assessing the relationship between points. It is important to note that, during the process of clustering, the relationships between the remaining points in the cluster and the points to be measured are ignored. In consideration of the aforementioned issues, this paper proposes the utilization of extension distance for the purpose of evaluating the relationship between the points to be measured and the cluster classes. Furthermore, it introduces a variant of the K-means algorithm based on the separator distance. Through a series of comparative experiments, the effectiveness of the proposed algorithm for clustering fan-shaped datasets is preliminarily verified.

Keywords: clustering; extenics; extension distance

MSC: 62H30; 03B52

Academic Editor: Simeon Reich

Received: 12 July 2025
Revised: 28 July 2025
Accepted: 30 July 2025
Published: 6 August 2025

Citation: Li, X.; Yue, H.; Qin, Y.; Zhang, H. Extension Distance-Driven K-Means: A Novel Clustering Framework for Fan-Shaped Data Distributions. *Mathematics* **2025**, *13*, 2525. https://doi.org/10.3390/math13152525

1. Introduction

The K-means algorithm is regarded as a classic in the field of clustering. It employs the Euclidean distance metric to quantify the similarity between data points. The primary advantages of this approach are twofold [1]: firstly, it exhibits high computational efficiency and, secondly, it provides strong interpretability of clustering results. However, the methodology is not without its drawbacks, which include high-dimensional failure due to the breakdown of Euclidean distance metrics in sparse spaces [2], sensitivity to initialization centers leading to suboptimal local minima, susceptibility to outliers that disproportionately distort cluster centroids, and the inherent tendency to form isotropic spherical clusters [3], which fundamentally limits its applicability to complex geometries like fan-shaped distributions.

To mitigate these limitations, extensive research has explored alternative strategies.

Topology-aware methods like spectral clustering [3] leverage graph theory to capture non-convex structures. Dimensionality reduction techniques [4–6] project data into latent spaces where Euclidean assumptions hold more robustly. Distance metric adaptations, such as Manhattan distance [7,8] and specialized similarity measures [9,10], aim to reduce sensitivity to outliers and high-dimensional noise.

While these approaches improve performance in specific scenarios [11–13], they often neglect intra-cluster relational dynamics. Specifically, during assignment, the similarity computation remains centroid-centric, ignoring interactions between the target point and other members of the cluster. This oversight is critical in fan-shaped distributions where radial density and angular relationships define cluster cohesion.

Recent grid-based optimizations enhance scalability but do not fundamentally address the centroid-centric bias. For instance, Yang et al. [14] accelerated center selection via spatial grid partitioning, while Moghaddam et al. [15] optimized device-to-device clustering using social-physical features. Though efficient, these methods still rely on point-to-centroid distances.

Our work bridges this gap by proposing an extension distance framework that explicitly incorporates intra-cluster relationships through set-based similarity metrics, enabling adaptive learning of fan-shaped geometries.

2. Extension Distance

2.1. One-Dimensional Extension Distance

In classical mathematics, distance is commonly used to measure the relationship between points and intervals. In the event that the point under consideration falls within the interval, the distance is deemed to be zero. However, it should be noted that this does not serve to differentiate between different points within the same interval. In order to differentiate between disparate points within a given interval and the interval itself, extenics [16] is introduced in the extension distance. This concept describes the positional relationship between any point and a fixed point x_0 and an interval $X = \langle a, b \rangle$. If the fixed point x_0 in the internal $X = \langle a, b \rangle$ is located at the midpoint of the interval, the extension distance is:

$$p_m(x, x_0, X) = \left| x - \frac{a+b}{2} \right| - \frac{b-a}{2} = \begin{cases} a - x, x \leq \frac{a+b}{2} \\ b - x, x \geq \frac{a+b}{2} \end{cases} \tag{1}$$

Equation (1) delineates the relationship between point x and the interval with fixed point x_0 at the midpoint of the interval (the open or closed nature of the interval in the expandable distance is flexibly altered according to the actual situation; hence, the above symbols are used to represent the interval). The subsequent illustration employs the midpoint extension distance to demonstrate its values.

As shown in Figure 1, let X be an interval. The point x of the extension distance $p_m(x, x_0, X)$ relative to the center of interval $X = \langle 2, 4 \rangle$ is shown in Figure 1. When point x is outside the interval, the value of the middle extension distance $p_m(x, x_0, X)$ is greater than zero, and the further point x is from the center of the interval, the greater the value of $p_m(x, x_0, X)$. When point x is inside the interval, $p_m(x, x_0, X)$ takes its minimum value. The values of the left and right extension distances are as described in the extenics; due to space constraints, these are not detailed here.

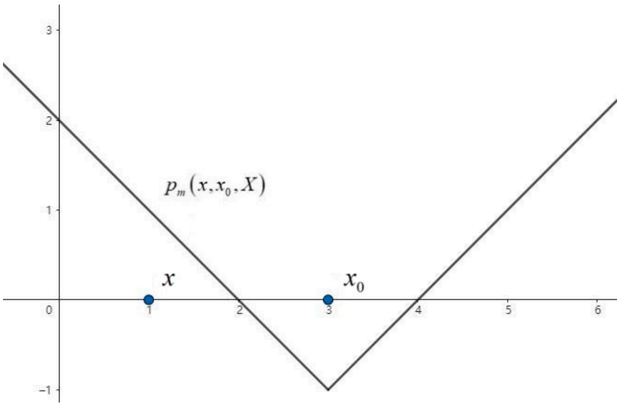

Figure 1. Schematic diagram of extension distance.

2.2. Limitation in High Dimensions

As mentioned above, the extension distance can accurately depict the relationship between points and intervals in one dimension. However, most datasets in the field of data analysis are high-dimensional. While applying the extension distance to analyze multiple one-dimensional datasets can leverage its advantages in describing points and intervals, this approach overlooks the interdependencies between data across different dimensions. Therefore, the one-dimensional extension distance is not adequate for data analysis purposes. The concept of the kernel radius has therefore been extended to two dimensions. Feature planes are formed through the pairwise combination of all dimensions in a high-dimensional dataset, and a two-dimensional kernel radius is then applied to analyze these planes. This approach retains the kernel radius's original advantage in describing points and intervals, while mitigating the issue of neglecting inter-dimensional data correlations inherent in the one-dimensional kernel radius.

3. Extension Distance in Two-Dimensional Space

3.1. Straight Line Traversal Method

We first propose using the straight line traversal method to calculate the extension distance in two-dimensional space [17]. This method is used to calculate the extension distance between the midpoint of the plane and the set.

As shown in Figure 2a, there is a point e and a set D in a two-dimensional plane. To calculate the extension distance between point e and set D, first draw a straight line through set D that passes through point e. According to Equation (1), the extension distance between point e and the points on this line that belong to set D can then be calculated as follows:

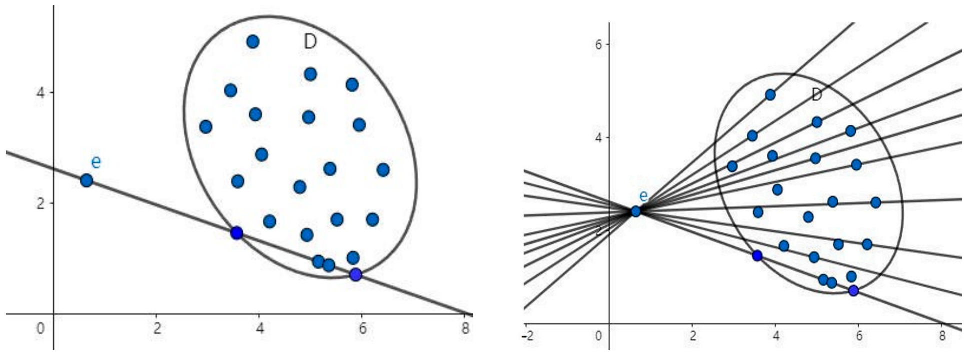

(**a**) (**b**)

Figure 2. (**a**) Schematic diagram of straight line traversal calculation. (**b**) Schematic diagram of line traversal calculation set D.

$$\begin{aligned} p_x &= p_m\left(x_e, \frac{x_{min}+x_{max}}{2}, [x_{min}, x_{max}]\right)\frac{n}{s} \\ p_y &= p_m\left(y_e, \frac{y_{min}+y_{max}}{2}, [y_{min}, y_{max}]\right)\frac{n}{s} \end{aligned} \quad (2)$$

According to Equation (2), the extension distances p_x and p_y of point e on the x and y axes, respectively, relative to the aforementioned intervals are calculated. Equation (2) represents the projection of all points onto the x and y axes, forming the internals $[x_{min}, x_{max}]$ and $[y_{min}, y_{max}]$ by points belonging to set D. Finally, the proportion of the extension distance corresponding to the straight line is calculated in relation to the total extension distance $(p(e, D))$ using the weight n/s (where n denotes the number of points on the line belonging to the set and s denotes the total number of points in set D). Note that when only one point on the line belongs to set D, all extension distances are greater than zero according to Equation (1), still satisfying the property that points outside the interval have extension distances greater than zero. As shown in Figure 2b, when all lines completely traverse the set, the extension distance of point e relative to set D can be obtained. The extension distance of set D can be calculated using the following Equation (3).

3.2. Properties and Verification

Here, w_x and w_y represent the weights of the extension distances in the x and y directions, respectively. Their values are determined according to the actual situation.

$$\begin{gathered} p_x(e,D) = \sum_{t=1}^{t} p_m\left(x_e, \frac{x_{min}+x_{max}}{2}, [x_{min}, x_{max}]\right)\frac{n}{s} \\ p_y(e,D) = \sum_{t=1}^{t} p_m\left(y_e, \frac{y_{min}+y_{max}}{2}, [y_{min}, y_{max}]\right)\frac{n}{s} \\ p(e,D) = w_x p_x(e,D) + w_y p_y(e,D) \end{gathered} \tag{3}$$

For the purposes of illustration, consider Figure 3. Point e exhibits three distinct positional relationships with set D: the point is outside the set, the point is on the edge of the set, and the point is inside the set.

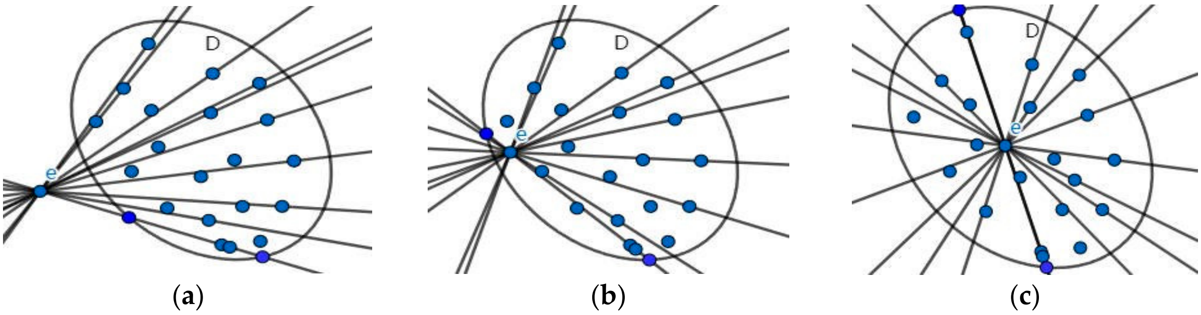

(**a**) (**b**) (**c**)

Figure 3. (**a**) Point outside the set. (**b**) Point on the edge of the set. (**c**) Point inside the set.

- In the event of point e lying outside set D, for any line passing through the set such that $x_e \notin [x_{min}, x_{max}]$ and $y_e \notin [y_{min}, y_{max}]$ is satisfied, it follows that for any of the above lines, p_x and p_y are greater than 0. Consequently, $p(e,D)$ is greater than 0. The following essay will provide a comprehensive overview of the relevant literature on the subject.
- When point e is on the boundary of set D, for any line passing through the set, $x_e = x_{min}$ or $x_e = x_{max}$, then for any of the above lines, p_x and p_y are both equal to 0, so $p(e,D)$ is equal to 0.
- In the event of point e being in set D, for any line passing through the set such that $x_{min} < x_e < x_{max}$ and $y_{min} < y_e < y_{max}$, it can be concluded that $p(e,D)$ is less than 0.

In summary, upon expanding the extension distance to a two-dimensional plane, it is observed that the numerical values and meanings remain consistent with the original extension distance, as systematically categorized in Table 1.

Table 1. The extension distance between point and intervals or sets.

The Positional Relationship Between Points and Intervals or Set	Extension Distance Between Point and Interval	Extension Distance Between Point and Two-Dimensional Plane Set
Point outside the interval or set	$p(x, x_0, X) > 0$	$p(e, D) > 0$
Point on the edge of the interval or set	$p(x, x_0, X) = 0$	$p(e, D) = 0$
Point inside the interval or set	$p(x, x_0, X) < 0$	$p(e, D) < 0$

3.3. Fixed-Angle Traversal Method

As demonstrated above, the method can be extended to a two-dimensional plane in order to describe the relationship between a point and a set. However, in practical applications, the line traversal method is too strict in terms of data point distribution and involves a high number of calculation steps, due to the varying distribution of data points. It is evident that the angle traversal method is further adopted to enhance calculation efficiency. As demonstrated in Figure 4, traversing the set D from a point using a fixed angle α not only reduces the requirements for data point distribution but also improves traversal computation efficiency.

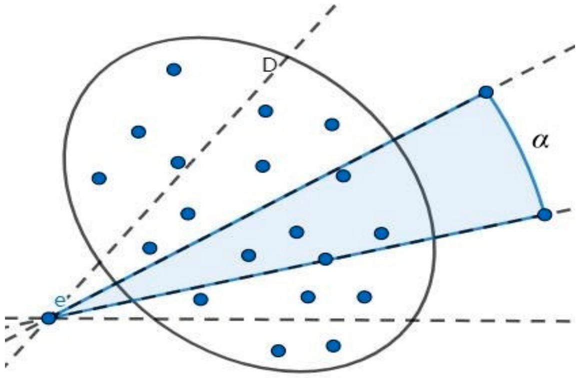

Figure 4. Schematic diagram of traversing a set at an angle.

3.4. Verification and Set Intersection

In light of the modification to the traversal method, it is imperative to undertake a re-verification of the extended distance calculation outcomes, ensuring their congruence with the established spatial relationships.

As shown in Figure 5a, point e is located outside set D. There are three possible scenarios when traversing the set at a fixed angle.

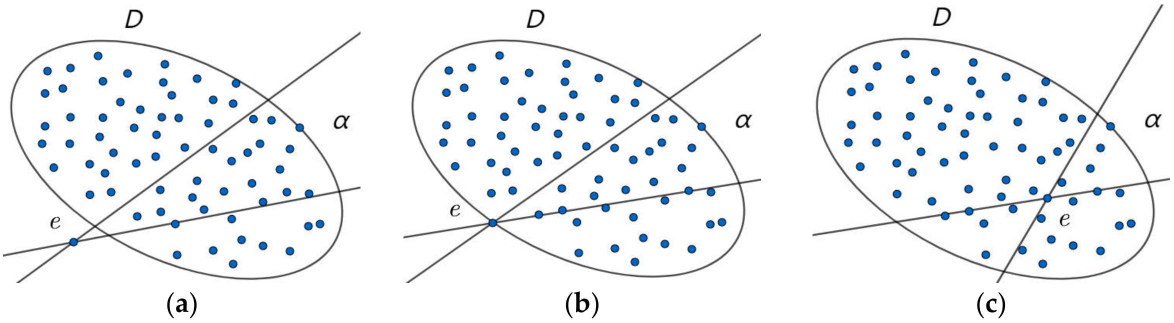

Figure 5. (**a**) Point outside the set. (**b**) Point on the edge of the set. (**c**) Point inside the set.

- In Scenario 1, only one point belongs to the set D within the fan-shaped range. Furthermore, interval $X = \langle a_x, b_x \rangle$ is a single point and $a_x = b_x$, so we have:

$$\begin{aligned} p_x &= \left| e_x - \tfrac{a_x+b_x}{2} \right| - \tfrac{b_x-a_x}{2} = |e_x - a_x| > 0 \\ p_y &= \left| e_y - \tfrac{a_y+b_y}{2} \right| - \tfrac{b_y-a_y}{2} = |e_y - a_y| > 0 \end{aligned} \tag{4}$$

The derivation in Equation (4) demonstrates that when only one point exists in the sector, the extension distances p_x and p_y remain strictly positive, confirming the external position property.

- In Scenario 2: There are two or more points in the sector belonging to set D and none of the sector boundaries are vertical or horizontal. According to Figure 1, we know that, for the interval $X = \langle a_x, b_x \rangle, a_x \neq b_x$, so $p(e, D) > 0$.
- In Scenario 3: There are two or more points within the sector belonging to set D and a horizontal or vertical sector edge. In this case, projecting the obtained points onto the x or y axis results in a single point rather than an interval, so $e_x = a_x = b_x$ or $e_y = a_y = b_y$. According to Equation (3), analyzing the case where $e_x = a_x = b_x$ gives us $p(e, D) > 0$.

This discussion does not cover cases where one side of the sector is horizontal and the other is vertical, since the corresponding fixed angle α would be too large under such conditions. Excessively large a values cause calculation errors in practical applications. In summary, when point e lies outside set D, the extension distance $p(e, D)$ is greater than zero if Equation (3) is used with a smaller, more reasonable fixed angle α to traverse the set.

Similarly, it is straightforward to demonstrate that both points on the edge of the set (Figure 5b) and points within (Figure 5c) satisfy the original quantitative relationship.

In summary, after changing the traversal method, the results of the extension distance calculation still maintain consistency with the position relationship. However, further verification is needed for the problem of points and multiple sets. For example, if the distance between point e and sets D and F is less than 0, then sets D and F must intersect.

To verify the above problem, assume that point E is located at the intersection of sets D and F. According to the preceding proof:

$$\begin{aligned} p(e, D) = w_x p_x(e, D) + w_y p_y(e, D) < 0 \\ p(e, F) = w_x p_x(e, F) + w_y p_y(e, F) < 0 \end{aligned} \tag{5}$$

The simultaneous conditions in Equation (5) establish a necessary foundation for proving set intersection under negative extension distances.

Taking the x-axis as an example, sets D and F both have intervals $X_D = \langle a(x, D), b(x, D) \rangle$ and $X_F = \langle a(x, F), b(x, F) \rangle$ such that the x-coordinate of point e satisfies the following quantitative relationship:

$$\begin{aligned} a_{x,D} < x_e > b_{x,D} \\ a_{x,F} < x_e > b_{x,F} \end{aligned} \tag{6}$$

As quantified in Equation (6), the coordinate containment relationships provide direct evidence for interval overlap on each axis dimension.

It is evident that the intervals X_D and X_F on the x axis overlap if they encompass the same set of points. The same applies to the y axis. Finally, it is evident that sets D and F intersect within the two-dimensional plane.

4. K-Means Variant Based on Extension Distance

4.1. Limitations of Standard K-Means

The K-means clustering algorithm is chiefly reliant upon the utilization of the Euclidean distance metric to ascertain the similarity between data points. The purpose of this process is to repeatedly calculate and compare the distances between the remaining points in the dataset and the initial k center points until the sum of these distances is minimized. The objective function is as follows [18]:

$$J = \sum_{j=1}^{k} \sum_{i=1}^{s} \left\| x_i^{(j)} - c_j \right\|^2 \tag{7}$$

As demonstrated in the above formula, the affiliation relationship between the measured point and the cluster class is contingent on its Euclidean distance to each center point. In each calculation, the measured point is classified as the center point with the closest distance. Subsequent to the calculation of the data set, the coordinates of each cluster class are recalculated to obtain new center points, whereupon a new round of clustering commences. The aforementioned steps are to be repeated until the center points stabilize. Despite the fact that the K-means algorithm is capable of rapidly and directly obtaining clustering results in a dataset, during the classification process, the algorithm solely considers the relationship between the data points and the cluster centers, disregarding the influence of other points within the cluster on the classification of the data points. Despite the utilization of the mean coordinate calculation method in the subsequent update of the cluster centers, thereby augmenting the influence of the residual points within the cluster on the cluster centers, the fundamental process of directly determining the cluster classification of the data points remains predicated on a solitary method of point-to-point distance, a method that is encumbered by certain limitations.

Furthermore, by leveraging angular relationships, our fixed-angle traversal method significantly reduces computational complexity. Compared to traditional Euclidean distance calculations $(O(n^2))$, the angular-based approach optimizes traversal to $O(n \cdot k)$ (where k is the number of angles), enabling faster clustering for fan-shaped distributions.

4.2. Proposed Algorithm Framework

In the context of K-means clustering, two primary types exist: (1) the standard type with a predefined number of clusters n, where the algorithm partitions data into n clusters by minimizing within-cluster variance; and (2) an alternative type with no predefined cluster count but a predefined threshold for the minimum number of elements per cluster, allowing the number of clusters to emerge dynamically based on this threshold. Our proposed algorithm strictly adopts the first type, with n (the number of clusters) provided as an input parameter. We do not incorporate the second type or its threshold-based mechanism, as our focus is on enhancing clustering accuracy for fan-shaped distributions through extension distance, without automatic cluster number determination.

In order to address this issue, the present paper proposes a methodology based on the K-means algorithm that uses a two-dimensional extension distance to calculate the similarity between the points to be measured and the cluster classes, thereby determining the cluster class to which each point belongs. In order to calculate the similarity between the unknown points and the cluster classes, the two-dimensional extension distance method is employed to divide and traverse each cluster class in a fan shape with a fixed angle α based on the unknown points. This approach ensures that the influence of each point within the cluster on the similarity of the unknown points during the classification process is comprehensively considered. In practical applications, the data sets are usually multidimensional, but the two-dimensional extension distance is limited to two-dimensional plane problems. In order to address this issue, a feature recombination method is adopted. In the context of data sets characterized by n features, these features are arranged in pairs to yield C_n^2 feature planes, which are subsequently calculated. Notwithstanding the fact that C_n^2 is substantial when the dataset under consideration contains a considerable number of features, the algorithm is required to perform calculations on multiple planes, thereby increasing the computational load. Furthermore, the method of permuting and combining features to obtain feature planes is only capable of considering the correlation between two features and is unable to analyze the intrinsic relationships among three or more features. However, even when processing datasets on a two-dimensional plane, the algorithm is able to consider the interactions between different features in multidimensional datasets, thereby partially accounting for the intrinsic relationships among features.

The detailed process of the proposed clustering algorithm based on two-dimensional extension distance is outlined in Algorithm 1. This algorithm integrates the extension distance metric with angular traversal to optimize fan-shaped data clustering.

Algorithm 1: Extension-Distance-Driven K-means Clustering

```
Input: dataset $S$, clusters $n$, angle $\alpha$
Calculate the distance maxima: $min(D)$, $max(D)$
Calculate $P_l^{(i,j)}$, $P_r^{(i,j)}$, $\overline{P}_l$, $\overline{P}_r$ [19]
for $i$ in $\left[min\left(P_l^{(i,j)}\right)\ldots max\left(P_l^{(i,j)}\right)\right]$ do
    if $i > \overline{P}_r$ then
        Set the point corresponding to $i$ as centroid $c_1$
        Break
    end if
end for
repeat
    $P_{temp}$ = Randomly select from $\left[i\ldots max\left(P_l^{(i,j)}\right)\right]$
    $c_{temp}$ = The corresponding point to $P_i$
if all $P_l^{(c_{temp},c_i)} > \overline{P}_r$ then
        set $P_{temp}$ as the centroid
    end if
until Number of centres meets requirements
repeat
Precompute angular relation matrix A(Equation (1)) to store relative angles between all points
Utilize A to accelerate fixed-angle traversal, reducing redundant calculations.
    for $i\_simple$ in $S$ do
        for $i\_plane$ in [$plane_1\ldots plane_e$] do
            for $i\_cluster$ in all cluster do
                Calculate $P_{i\_plane,i\_cluster}$
                end for
                $P_{i\_cluster} = \sum P_{i\_plane,i\_cluster}$
                $i\_simple$ belong to $i\_cluster$ corresponding to min($P_{i\_cluster}$)
            end for
        end for
        For each cluster, find the sample corresponding to min($P_{i\_cluster}$)
    until Centre point remains stable
```

4.3. Angle Relation Matrix

It is imperative to note that this algorithm employs a predetermined angle α fan shape to traverse the cluster class and calculate the extension distance. In order to circumvent the repetition of calculations and enhance efficiency, it is essential to ascertain the relative angles between each point on the plane prior to calculating the extension distance on the feature plane.

As demonstrated in Figure 6, the relative angles between two points, e and h, on a plane exhibit a quantifiable relationship, as outlined below:

$$\varepsilon = \begin{cases} \beta + \pi, \beta \leq \pi \\ \beta - \pi, \beta \geq \pi \end{cases} \tag{8}$$

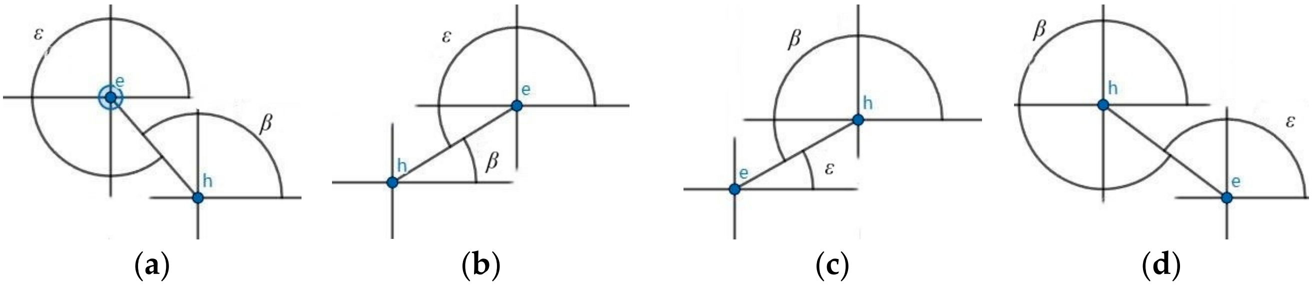

Figure 6. (**a**) Relative positional relationship between points 1. (**b**) Relative positional relationship between points 2. (**c**) Relative positional relationship between points 3. (**d**) Relative positional relationship between points 4.

Therefore, for any two points in the feature plane, it is only necessary to determine the relative angle between point e and point h. Then, according to Equation (8), the relative angle between point h and point e can be calculated, and finally, an $n \times n$ relative angle square matrix can be obtained. In the context of the algorithm, the term 'relative angle' is defined as the angle between the n th point in the data set and the first point. It has been established that there exists a quantitative relationship between the relative angle and the parameter $\beta_{(n,1)}$. Consequently, the calculation of the upper or lower half of the matrix during operation is sufficient to enhance the computational efficiency of the algorithm.

$$\begin{bmatrix} 0 & \cdots & \beta_{1,n} \\ \vdots & \ddots & \vdots \\ \varepsilon_{n,1} & \cdots & 0 \end{bmatrix} \tag{9}$$

The structured representation in Equation (9) achieves up to 50% storage reduction by leveraging the angular symmetry property formalized in Equation (8).

4.4. Complexity Analysis

We analyze the computational complexity of the proposed Extension–Distance-Driven K-means algorithm. The time complexity is dominated by two main components: the precomputation of the angle relation matrix and the iterative clustering process.

Precomputation of the angle relation matrix (Equation (9)): This involves calculating the relative angles between all pairs of points in the dataset, which requires $O(n^2)$ time, where n is the number of data points.

Iterative Clustering Process: For each iteration:

- The algorithm processes each data point (n points), each cluster (k clusters, where k is the number of clusters), and each feature plane. With d features, the number of feature planes is $C(d, 2) = O(d^2)$.
- For each combination, the fixed-angle traversal method with a number of angles a (related to the input angle α) is used. The traversal involves $O(a)$ operations per combination.
- Thus, the per-iteration complexity is $O(n \cdot k \cdot d^2 \cdot a)$

The total complexity per iteration is $O(n^2 + n \cdot k \cdot d^2 \cdot a)$. Since the angle relation matrix is computed once before iterations, and iterations are repeated until convergence (let T be the number of iterations), the overall complexity is $O(n^2 + T \cdot n \cdot k \cdot d^2 \cdot a)$.

In practice, with typical values, the dominant terms depend on parameters. For large n, the $O(n^2)$ term may be significant, but optimizations or parallel implementations can mitigate this. The parameters, such as k (number of clusters), d (dimensionality), and a (number of angles) affect the running time, and a should be chosen to balance accuracy and efficiency. The accepted accuracy can be tuned by adjusting α, with smaller angles increasing α and potentially improving accuracy, but at a higher computational cost.

5. Algorithm Comparison Experiment

5.1. Evaluation Metrics

The evaluation of clustering effectiveness is often contingent on specific practical requirements, and there is currently a paucity of strictly unified metrics for assessing the quality of clustering results. The selection of these metrics is driven by their complementary strengths in evaluating clustering performance for fan-shaped distributions. External metrics (ARI and NMI) are chosen because they measure the agreement between clustering results and ground-truth labels, providing a direct assessment of accuracy for synthetic datasets like ours with known distributions (e.g., the six-sector structure in Figure 7). This is crucial for validating geometric fidelity in complex non-spherical clusters. Internal metrics (DBI and Silhouette Score) are included to assess intra-cluster cohesion and inter-cluster separation without prior knowledge, offering insights into intrinsic cluster quality. However, we acknowledge their limitations in non-convex geometries—DBI may over-penalize irregular shapes, and Silhouette Score can underperform for anisotropic distributions—which aligns with our analysis in Section 5.4. This dual approach ensures a balanced evaluation, leveraging external metrics for objective validation and internal metrics for robustness checks in sparse or unlabeled scenarios. This study employs two commonly used internal metrics—the Davies–Bouldin Index (DBI) [20] and the Silhouette Score [21]—alongside two external metrics: the Adjusted Rand Index (ARI) [22] and Normalized Mutual Information (NMI) [23]. These internal metrics operate without prior knowledge of true cluster distributions, relying solely on intra-cluster compactness and inter-cluster sparsity for evaluation.

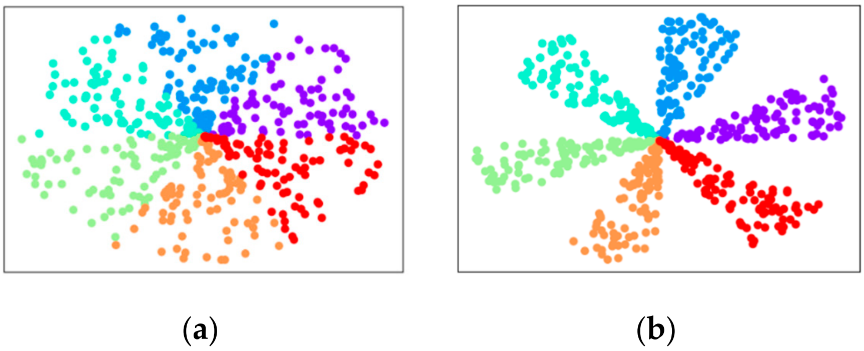

Figure 7. (**a**) Dataset A. (**b**) Dataset B. **Color legend**: Blue, green, red, orange, purple, and cyan points represent the six distinct ground-truth clusters.

In order to verify the feasibility of the algorithm, it was compared with common clustering algorithms and the algorithm before improvement through experiments. The distribution of the data sets utilized in the experiment is illustrated in Figure 7. Each data set contains 300 sample points, which are uniformly divided into six clusters.

5.2. Datasets and Experimental Setup

To verify the algorithm's feasibility, it was compared with common clustering algorithms and the unimproved version through experiments. The dataset distributions used in the experiments are shown in Figure 7. Each dataset contains 300 sample points, uniformly divided into six clusters.

5.3. Clustering Results Visualization

The clustering results of the algorithms for datasets A and B are shown in Figure 8. In the context of dataset A, both the enhanced algorithm and conventional clustering algorithms, such as GMM, encounter a similar predicament: they are unable to effectively differentiate between the closest points within clusters. The center of the dataset was erroneously designated as belonging to a single cluster; however, in reality, this location is where the points from multiple clusters are most densely distributed. Due to the erroneous classification of the center as a single cluster and the initial number of clusters being set to six, these algorithms are required to divide the remaining sample points surrounding the center into five clusters, despite the fact that they actually belong to six clusters. The sequence of errors initiated by the erroneous categorization of the dataset center results in suboptimal clustering efficacy of the aforementioned algorithms on dataset A. Despite the limitations of the proposed algorithm in this paper in fully restoring the genuine proportions of each cluster type in dataset A to a high degree, as demonstrated in Figure 8 in comparison to the true distribution of data A in Figure 7a, the cluster type proportions corresponding to the purple and cyan regions are comparatively diminutive, whilst those corresponding to the blue, green, and orange regions are comparatively substantial. Furthermore, the central segment of dataset A was originally distributed across six cluster points. However, following clustering by the algorithm, only four cluster points remained in the central segment, resulting in some cluster points being incorrectly classified in the central region of dataset A. Nevertheless, the algorithm reasonably reproduces the distribution trends of the clusters: six clusters are distributed in a fan-shaped pattern within a circular dataset.

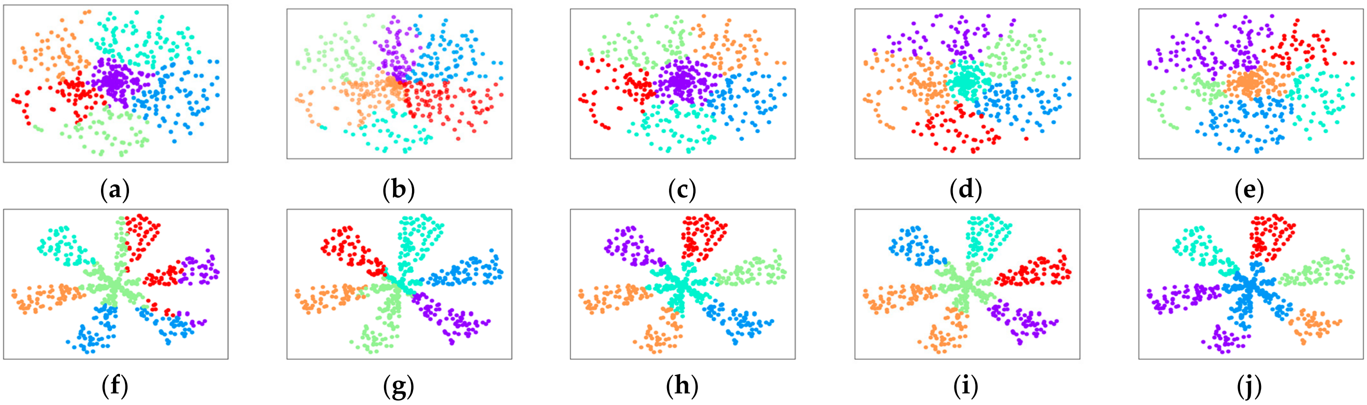

Figure 8. (**a**) Results of algorithm before improvement on dataset A. (**b**) Results of the proposed algorithm on dataset A. (**c**) Results of K-means ++ on dataset A. (**d**) Results of GMM on dataset A. (**e**) Results of Agglomerative on dataset A. (**f**) Results of algorithm before improvement on dataset B. (**g**) Results of the proposed algorithm on dataset B. (**h**) Results of K-means ++ on dataset B. (**i**) Results of GMM on dataset B. (**j**) Results of Agglomerative on dataset B. **Color legend**: Each color represents a distinct cluster label assigned by the corresponding algorithm.

Dataset B is a simplified version of dataset A. The six clusters are distributed in a circular dataset in a fan-shaped pattern, but in dataset B, the clusters only touch each other in the center. There are also certain blank areas on both sides of each cluster's fan shape.

Notwithstanding this fact, the conventional clustering algorithms continue to generate the same error as with dataset A: they categorize the center of dataset B as a solitary cluster. In a similar manner, the remaining sample points surrounding the central part of dataset B are to be divided into five clusters by these algorithms. However, in reality, there are six clusters. It is evident that, due to the presence of blank intervals between the clusters in dataset B, the clustering errors of the algorithm are more pronounced in Figure 8. To illustrate this, the clustering results of dataset B, obtained using the improved algorithm, were analyzed. It was found that the algorithm incorrectly classified the central part of dataset B into a single cluster. This resulted in a chain reaction that necessitated the division of the remaining six sector parts into five clusters. As is evident in the figure, the red clusters are distributed across three sector regions, while the purple and blue clusters are distributed across two sector regions. However, in dataset B, it was found that each sector region corresponded to only one color cluster. The erroneous categorization of the central element invariably results in erroneous cluster divisions in subsequent iterations of the algorithm. Despite the enhanced algorithm's inability to adequately segment the primary component of dataset B, the central portion—comprising six distinct clusters—is successfully divided into clusters that correspond to the blue and green categories. Additionally, a segment of the green cluster exhibits a transition into the orange cluster. However, the clustering results of the proposed algorithm for dataset B demonstrate a superior reproduction of the distribution of clusters in dataset B in comparison to other algorithms (Figure 8g).

5.4. Quantitative Results Analysis

The results of evaluating the clustering performance of various algorithms on datasets A and B using two external and internal metrics are shown in Tables 2 and 3. It is evident that, among these metrics, external metrics ARI and NMI indicate a close correlation between the proximity of their values to 1 and the extent to which the clustering results align with the true cluster distribution. The internal metric Silhouette Score indicates that the closer its value is to 1 and the closer DBI is to 0, the better the clustering: each cluster is well-defined, with tight internal cohesion and significant separation between clusters.

Table 2. Dataset A clustering results on the evaluation of clustering metrics.

Algorithm	ARI	NMI	Silhouette Score	DBI
Algorithm before Improvement	0.304	0.480	0.329	0.904
This article's algorithm	0.480	0.597	0.259	0.974
K-means ++	0.289	0.485	0.388	0.794
GMM	0.383	0.526	0.346	0.860
Agglomerative	0.305	0.478	0.330	0.854

Table 3. Dataset B clustering results on the evaluation of clustering metrics.

Algorithm	ARI	NMI	Silhouette Score	DBI
Algorithm before Improvement	0.328	0.529	0.354	0.855
This article's algorithm	0.658	0.736	0.367	0.927
K-means ++	0.378	0.604	0.473	0.732
GMM	0.389	0.610	0.471	0.732
Agglomerative	0.395	0.617	0.453	0.760

Notably, the grid-based acceleration in [14] achieved 80% time reduction on 100k-scale datasets by replacing point-level computations with cell density metrics. Although our focus is on fan-shaped geometry adaptation rather than scalability, this demonstrates the potential of hybridizing the extension distance method with grid strategies. Meanwhile, Ref. [15] proposes social-aware clustering method achieved 70% throughput gain, aligning with our observation that intra-cluster relationships impact performance.

As demonstrated in the above tables, the proposed algorithm in this paper demonstrates superior performance in terms of external metrics when compared to other algorithms. This finding is further substantiated by the clustering results presented in Figure 8, which illustrate that, under the true distribution of the reference dataset, the proposed algorithm can effectively cluster and reproduce the true shape of the dataset, in contrast to the performance of other algorithms. However, the implementation of alternative algorithms has been observed to result in the erroneous classification of clusters within the central region of the dataset. This has been shown to precipitate a sequence of cascading reactions, resulting in a significant deviation of the clustering outcomes from the underlying true distribution of the dataset. This issue is also reflected in external metrics based on the true labels of the dataset, particularly in the ARI metric, where other algorithms perform significantly worse than the proposed algorithm. With regard to internal metrics such as the Silhouette Score and DBI, the proposed algorithm demonstrates suboptimal performance. This is particularly evident in the DBI metric, where, despite the proposed algorithm exhibiting a reduced gap in comparison to alternative algorithms, it nevertheless achieves a lower ranking. This phenomenon may be attributed to one of the limitations inherent in the DBI: It is evident that there is a deficiency in the robustness of the system with regard to non-spherical or non-circular clusters, which may result in erroneous evaluations. The clustering results of the present algorithm for datasets A and B manifest as fan-shaped, and similarly, due to the non-spherical and non-circular nature of the clusters, the present algorithm also performs poorly on the internal metric Silhouette Score. Despite the fact that the proposed algorithm performs inadequately in terms of the two internal metrics, the disparities between the algorithms in the experiments are less pronounced in the internal metrics than in the external metrics. Through experimentation on datasets A and B, the effectiveness of the proposed algorithm in handling fan-shaped distribution datasets has been verified.

6. Discussion

The present paper puts forward a variant of the K-means clustering algorithm based on extension distance, which has been validated through comparative experiments on two datasets with fan-shaped distribution characteristics. However, further research is required to analyze the factors influencing the extension distance clustering algorithm.

Based on the experimental results from Section 5 (Tables 2 and 3), we infer that these factors significantly influence the algorithm's robustness. For instance, increasing the number of clusters beyond six (as tested) may degrade the Adjusted Rand Index (ARI) due to higher overlap in fan-shaped distributions, particularly in the central regions of datasets like A and B. Similarly, sparse data distributions (e.g., with larger inter-cluster gaps in dataset B) could improve the Silhouette Score by enhancing separation, whereas compact distributions may increase the Davies–Bouldin Index (DBI) due to reduced intra-cluster cohesion. Future work should include controlled experiments varying the cluster count (e.g., k = 4 to 10), data size (e.g., n = 100 to 1000 points), and sparsity levels (e.g., by adjusting the angular spread or density) to quantify these effects comprehensively. This would provide deeper insights into the algorithm's scalability and applicability to diverse real-world scenarios. Notably, the current experiments utilize datasets of 300 points each. While this scale suffices for validating the core fan-shaped clustering capability, larger datasets (e.g., >10,000 points) may impact computational efficiency due to the $O(n^2)$ complexity of angle-relation matrix precomputation (Equation (9)).

Regarding the suboptimal performance on internal metrics such as the Silhouette Score and Davies–Bouldin Index (DBI), we attribute this primarily to the inherent limitations of these metrics in evaluating non-spherical cluster geometries. As demonstrated in Section 5.4, the Silhouette Score and DBI are optimized for isotropic, spherical clusters where intra-cluster compactness and inter-cluster separation are uniformly distributed. However, our algorithm targets fan-shaped distributions characterized by anisotropic structures and radial density variations, which violate the spherical assumption. Consequently, these metrics may misrepresent cluster quality—for instance, by penalizing the natural angular spreads in fan-shaped clusters as poor cohesion. Similarly, the lack of robustness for non-spherical or non-circular clusters stems from the algorithm's reliance on fixed-angle traversal (Section 3.3) and feature plane recombination (Section 4.2), which may not fully capture complex boundaries in irregular shapes. To address this, future enhancements could integrate adaptive angle mechanisms or extend the extension distance framework to non-convex sets. Future work will explicitly test scalability across varying data sizes.

Meanwhile, clustering algorithms based on two-dimensional extension distance involve the setting of two initial variables: the scanning angle and the number of clusters. Of these, the scanning angle has been demonstrated to have a significant impact on the clustering results. At this juncture, further exploration is required into the establishment of a reasonable scanning angle and the influence of the scanning angle on the clustering results. In summary, the proposed extension distance-based K-means variant successfully overcomes the spherical clustering limitation of traditional K-means by incorporating the relationships within clusters, as validated through comparative experiments on fan-shaped datasets (Figures 7 and 8). This approach enhances clustering accuracy for non-spherical distributions, particularly in scenarios with high inter-cluster sparsity. However, the identified limitations, such as sensitivity to the scanning angle and non-convex set handling, warrant further investigation to broaden applicability. Overall, this work provides a robust framework for fan-shaped data clustering, with potential extensions to other non-Euclidean distance metrics in future studies.

7. Conclusions

This study introduced a novel K-means variant based on the extension distance, designed to address the limitations of traditional spherical clustering in fan-shaped data distributions. By leveraging the extension distance metric, the algorithm incorporates intra-cluster relationships, enabling more accurate clustering for non-spherical datasets, as demonstrated through rigorous experiments on benchmark fan-shaped datasets (datasets A and B). Key findings include:

- The proposed algorithm significantly outperforms conventional methods (e.g., K-means ++, GMM) in external metrics such as ARI and NMI, highlighting its robustness for fan-shaped distributions.
- The two-dimensional extension distance framework effectively handles inter-feature correlations, overcoming the high-dimensional limitations of one-dimensional approaches.
- However, challenges remain in optimizing the scanning angle parameter and extending the method to non-convex sets. Future work will focus on adaptive angle selection and applications to multi-modal datasets. Overall, this research contributes a scalable and interpretable clustering framework, with implications for fields such as image segmentation and anomaly detection.

Author Contributions: Conceptualization, X.L.; Methodology, H.Y.; Software, Y.Q.; Validation, Y.Q. and H.Z.; Formal analysis, H.Y. and H.Z.; Investigation, H.Y.; Data curation, Y.Q.; Writing—original draft, H.Y.; Writing—review & editing, X.L.; Visualization, Y.Q.; Supervision, X.L.; Project administration, X.L. All authors have read and agreed to the published version of the manuscript.

Funding: This research was funded by National Natural Science Foundation of China: 72071049; GuangDong Basic and Applied Basic Research Foundation: 2024A1515011324.

Data Availability Statement: The original contributions presented in this study are included in the article. Further inquiries can be directed to the corresponding authors.

Conflicts of Interest: The authors declare no conflict of interest.

References

1. Yuan, C.; Yang, H. Research on K-value selection method of K-means clustering algorithm. *J* **2019**, *2*, 226–235. [CrossRef]
2. Aggarwal, C.C.; Hinneburg, A.; Keim, D.A. On the Surprising Behavior of Distance Metrics in High-Dimensional Space. In Proceedings of the 8th International Conference on Database Theory (ICDT 2001), London, UK, 4–6 January 2001; Van den Bussche, J., Vianu, V., Eds.; Springer: Berlin, Germany, 2001. Lecture Notes in Computer Science. Volume 1973, pp. 420–434.
3. Von Luxburg, U. A tutorial on spectral clustering. *Stat. Comput.* **2007**, *17*, 395–416. [CrossRef]
4. Ding, C.; He, X. Cluster Structure of K-means Clustering via Principal Component Analysis. In *Advances in Knowledge Discovery and Data Mining*; Dai, H., Srikant, R., Zhang, C., Eds.; Lecture Notes in Computer Science; Springer: Berlin, Germany, 2004; Volume 3056, p. 29.
5. Xu, Q.; Ding, C.; Liu, J.; Luo, B. PCA-guided search for K-means. *Pattern Recognit. Lett.* **2015**, *54*, 50–55. [CrossRef]
6. Feldman, D.; Schmidt, M.; Sohler, C. Turning Big Data into Tiny Data: Constant-Size Coresets for K-Means, PCA and Projective Clustering. In Proceedings of the Twenty-Fourth Annual ACM-SIAM Symposium on Discrete Algorithms (SODA '13), New Orleans, LA, USA, 6–8 January 2013; Society for Industrial and Applied Mathematics: Philadelphia, PA, USA, 2013; pp. 1434–1453.
7. Suwanda, R.; Syahputra, Z.; Zamzami, E.M. Analysis of Euclidean Distance and Manhattan Distance in the K-Means Algorithm for Variations Number of Centroid K. *J. Phys. Conf. Ser.* **2020**, *1566*, 012058. [CrossRef]
8. Wu, Z.; Song, T.; Zhang, Y. Quantum k-means algorithm based on Manhattan distance. *Quantum Inf. Process.* **2022**, *21*, 19. [CrossRef]
9. Singh, A.; Yadav, A.; Rana, A. K-means with Three different Distance Metrics. *Int. J. Comput. Appl.* **2013**, *67*, 13–17. [CrossRef]
10. Faisal, M.; Zamzami, E.M.; Sutarman. Comparative Analysis of Inter-Centroid K-Means Performance using Euclidean Distance, Canberra Distance and Manhattan Distance. *J. Phys. Conf. Ser.* **2020**, *1566*, 012112. [CrossRef]
11. Chen, L.; Roe, D.R.; Kochert, M.; Simmerling, C.; Miranda-Quintana, R.A. k-Means NANI: An Improved Clustering Algorithm for Molecular Dynamics Simulations. *J. Chem. Theory Comput.* **2024**, *20*, 5583–5597. [CrossRef] [PubMed]
12. Premkumar, M.; Sinha, G.; Ramkumar, M.D.; Ramakurthi, V. Augmented weighted K-means grey wolf optimizer: An enhanced metaheuristic algorithm for data clustering problems. *Sci. Rep.* **2024**, *14*, 5434. [PubMed]
13. Huang, W.; Peng, Y.; Ge, Y.; Kong, W. A new Kmeans clustering model and its generalization achieved by joint spectral embedding and rotation. *PeerJ Comput. Sci.* **2021**, *7*, 450. [CrossRef] [PubMed]
14. Yang, Y.; Zhu, Z. A Fast and Efficient Grid-Based K-means++ Clustering Algorithm for Large-Scale Datasets. In Proceedings of the Fifth Euro-China Conference on Intelligent Data Analysis and Applications (ECC 2018), Xian, China, 12–14 October 2018; Volume 891, pp. 485–495.
15. Moghaddam, S.S.; Ghasemi, M. Efficient Clustering for Multicast Device-to-Device Communications. In Proceedings of the 7th International Conference on Computer and Communication Engineering (ICCCE 2018), Kuala Lumpur, Malaysia, 19–20 September 2018; pp. 228–233.
16. Cai, W. Extension theory and its application. *Chin. Sci. Bull.* **1999**, *44*, 1538–1548. [CrossRef]
17. Qin, Y.; Li, X. A method for calculating two-dimensional spatially extension distances and its clustering algorithm. *Procedia Comput. Sci.* **2023**, *221*, 1187–1193. [CrossRef]
18. Lloyd, S. Least squares quantization in PCM. *IEEE Trans. Inf. Theory* **1982**, *28*, 129–137. [CrossRef]
19. Zhao, Y.; Zhu, F.; Gui, F.; Ren, S.; Xie, Z.; Xu, C. Improved k-means algorithm based on extension distance. *CAAI Trans. Intell. Syst.* **2020**, *15*, 344–351.425. [CrossRef]
20. Davies, D.L.; Bouldin, D.W. A cluster separation measure. *IEEE Trans. Pattern Anal. Mach. Intell.* **1979**, *1*, 224–227. [CrossRef] [PubMed]
21. Rousseeuw, P.J. Silhouettes: A graphical aid to the interpretation and validation of cluster analysis. *J. Comput. Appl. Math.* **1987**, *20*, 53–65. [CrossRef]
22. Hubert, L.; Arabie, P. Comparing partitions. *J. Classif.* **1985**, *2*, 193–218. [CrossRef]
23. Strehl, A.; Ghosh, J. Cluster ensembles—A knowledge reuse framework for combining multiple partitions. *J. Mach. Learn. Res.* **2002**, *3*, 583–617. [CrossRef]

Disclaimer/Publisher's Note: The statements, opinions and data contained in all publications are solely those of the individual author(s) and contributor(s) and not of MDPI and/or the editor(s). MDPI and/or the editor(s) disclaim responsibility for any injury to people or property resulting from any ideas, methods, instructions or products referred to in the content.